Breather trapping and breather transmission in a DNA model with an interface.

A Alvarez and FR Romero*
Grupo de Física No Lineal. Área de Física Teórica. Facultad de Física.
Universidad de Sevilla. Avda. Reina Mercedes, s/n. 41012-Sevilla (Spain)

JFR Archilla and J Cuevas
Grupo de Física No Lineal. Departamento de Fisica Aplicada I. ETSI Informática.
Universidad de Sevilla. Avda. Reina Mercedes, s/n. 41012-Sevilla (Spain)

PV Larsen
Department of Mathematics, Technical University of Denmark. DK-2800 Kgs. Lyngby (Denmark)
(Dated: March 24, 2006)

We study the dynamics of moving discrete breathers in an interfaced piecewise DNA molecule. This is a DNA chain in which all the base pairs are identical and there exists an interface such that the base pairs dipole moments at each side are oriented in opposite directions. The Hamiltonian of the Peyrard–Bishop model is augmented with a term that includes the dipole–dipole coupling between base pairs. Numerical simulations show the existence of two dynamical regimes. If the translational kinetic energy of a moving breather launched towards the interface is below a critical value, it is trapped in a region around the interface collecting vibrational energy. For an energy larger than the critical value, the breather is transmitted and continues travelling along the double strand with lower velocity. Reflection phenomena never occur.

The same study has been carried out when a single dipole is oriented in opposite direction to the other ones. When moving breathers collide with the single inverted dipole, the same effects appear. These results emphasize the importance of this simple type of local inhomogeneity as it creates a mechanism for the trapping of energy.

Finally, the simulations show that, under favorable conditions, several launched moving breathers can be trapped successively at the interface region producing an accumulation of vibrational energy. Moreover, an additional colliding moving breather can produce a saturation of energy and a moving breather with all the accumulated energy is transmitted to the chain.

I. INTRODUCTION

Nonlinear physics of DNA has experienced an enormous development in the previous years. There are many experimental data and theoretical results published about the nonlinear properties of DNA (for a review see, e.g., [1]. The DNA molecule is a discrete system consisting of many atoms having a quasi-one-dimensional structure. It can be considered as a complex dynamical system, and, in order to investigate some aspects of the dynamics and the thermodynamics of DNA, several mathematical models have been proposed. Among them, it is worth remarking the Peyrard–Bishop model [2] introduced for the study of DNA thermal denaturation. This model, and some variations of it, has also been used extensively for the study of the dynamical properties of DNA.

In DNA there exist different kinds of interactions between the main atomic groups. One of them is the stacking interaction between neighbouring bases along the DNA axis, these are short–range forces which stabilize the DNA structure and hold one base over the next one forming a stack of bases. There exist also long–range forces, due to the finite dipole moments of the hydrogen bonds within the nucleotides. The existence of these forces is corroborated both by theoretical and experimental studies. Recently, quantum chemical calculations, using the second Moler-Plesset perturbation method, have determined bonds lengths and bonds angles involved in hydrogen bonds between the bases of DNA base pairs, as well as dipole moments based at the MP2/6-31G(d) and MP2/6-31G(d,p) basis sets [3]. The dipole moments calculated for the adenine-thymine base pair at equilibrium are, respectively, 1.44 D and 1.29 D. The values calculated for the guanine-cytosine base pair at equilibrium are, respectively, 5.88 D and 5.79 D. All these

---

*Electronic address: romero@us.es

values are within the range of the parameters values for the dipole moments considered in this paper.

Some experiments carried out on the dynamics of the B-A transition of DNA double helices, through the analysis of the transients observed under electric field pulses, show that dipolar strectching is the main driving force for the B-A reaction [4].

The dipole–dipole interactions between different base pairs should never be ignored and they may play a crucial role for the dynamical properties of DNA, for example when the geometry of the double strand of DNA is taken into account, as the distance between base pairs and, therefore, the intensity of the coupling between them, depends on the shape of the molecule [5–11].

Most of the studies have been done considering DNA homogeneous models. Nevertheless, the DNA molecule is essentially an inhomogeneous system, and this inhomogeneity is characterized by the existence of different local ranges, or functional regions, with very specific sequences of base pairs and very specific functions.

Numerical simulations show that discrete breathers (DBs), which are spatially localized nonlinear oscillations, can appear in models of crystals, biomolecules, and many others nonlinear discrete systems [12–14]. It is well known that DBs can be static, but they can also move under certain physical conditions [15–17], constituting a mechanism for the transport of energy and information along discrete systems. They are called *moving breathers* (MBs) and have been obtained in many different systems [18–20].

In the Peyrard–Bishop model, the existence of DBs has been demonstrated [21, 22], and DBs are thought to be the precursors of the bubbles that appear prior to the transcription processes in which large fluctuations of energy have been experimentally observed [23].

The study of MBs in Klein-Gordon models of DNA chains with the inclusion of long–range interactions was initiated in [24] using an augmented Peyrard–Bishop model. The system considered is homogeneous and without bending, that is, all the base pairs are identical, aligned in a straight line, and all the dipole moments are parallel along the same direction. The results show that MBs exist for a wide range of the parameter values, although the mobility is hindered when the intensity of the long–range interaction increases. Essentially, the effective mass of a breather increases as the intensity of the dipole–dipole interaction increases, and there exists a threshold of the dipole–dipole coupling constant above which the breather is not movable.

The interaction of MBs with different kind of inhomogeneities in the DNA molecule may be also of great importance for the localization of energy [25, 26]. As a consequence of this interaction, MBs may be trapped in small regions, that is, vibrations remain affecting only to a small number of consecutive base pairs, producing an accumulation of energy, which can initiate denaturation or transcription bubbles. Also, trapping phenomena may be on the basis for the appearance of secondary breaks when DNA is irradiated with ionizing radiation [27].

Structural studies carried out with non coding sequences of DNA have shown that poly(dA.dT) sequences (called T-tracts) are abundant genomic DNA elements. Suter et al. [28]have shown that they exist as rigid DNA structures in nucleosome-free yeast promoters in vivo, that is, in vivo they are not folded in nucleosomes. Their data support that transcription activation depends on the length of the T-tracts and the same occurs when they are replaced by poly(dG.dC) sequences, another rigid structures. This fact suggests that the T-tracts operate not by recruitment of specific transcription factors, but rather by their intrinsic DNA structure, and that transcription activation must be intimately related with the dynamical properties of T-tracts.

These considerations motivated us to study MBs in some types of poly(dA.dT) or poly(dG.dC) sequences. In this paper we study the effects of the collisions of MBs with local inhomogeneities in two different but related systems.

The first system consists of an inhomogeneous DNA molecule formed by two consecutive homogeneous regions. All the base pairs are identical, but the dipoles of a region are oriented in opposite direction to the dipoles of the other one, as sketched in Fig. 1(a). One possibility is for a sequence being as $...AT/AT/AT/TA/TA/TA...$, where AT and TA represent, respectively, the adenine-thymine base pair and the thymine-adenine base pair. The other possibility is for a sequence being as $...CG/CG/CG/GC/GC/GC...$, where CG and GC represent, respectively, the cytosine-guanine base pair and the guanine-cytosine base pair. The inhomogeneity is determined by the existence of an interface that separates these regions, that is, there exists a local inhomogeneity and the interface marks a discontinuity in the system. These kind of chains are called *interfaced piecewise chains*, they exist in real DNA and can also be synthesized in the laboratory [29, 30].

The second system consists in a DNA chain of identical base pairs with all the dipoles oriented in the same direction, except one of them which has an opposite orientation, that is, the local inhomogeneity is at the site of the inverted–dipole, as sketched in Fig. 1(b).

In both systems, the simulations of MBs launched towards the inhomogeneity show that if the translational kinetic energy is below a critical value, which is determined by the values of the coupling parameters, the breather is trapped. For greater values, the breather is transmitted to the chain, losing part of its energy as phonon radiation. Moreover, reflection of the colliding breather never occurs.

These results emphasizes the enormous importance of a change of the orientation of a single base pair in a homogeneous track of DNA chain, as it demonstrates that a very simple structural change creates a mechanisms for
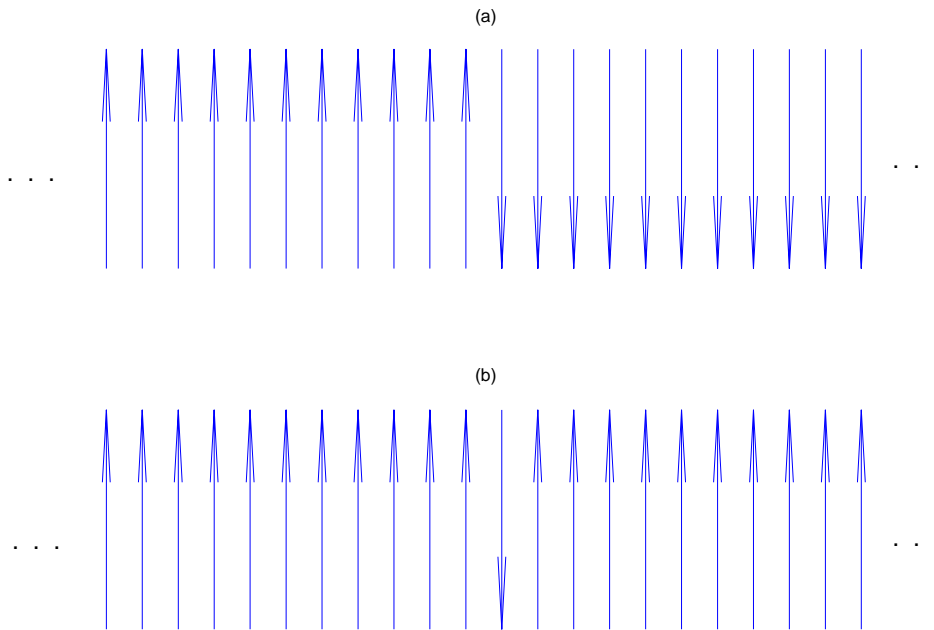
FIG. 1: Sketch of the dipole chains.(a): the interfaced piecewise chain, (b): the single inverted–dipole chain

localization and accumulation of energy.

Moving breathers can also collide with a trapped breather. Our study of these collision processes shows that multiple scenarios are possible, one of them is the possibility of getting an accumulation of energy at the interface up to a saturation threshold value. All the accumulated energy can be carried away by a successful incoming breather. These phenomena suggest a way for the DNA molecule to accumulate enough energy to break the hydrogen bonds between the base pairs on opposing strands.

Another important result concerning these systems, with a local inhomogeneity and with competing short and long–range interactions, is that there exists a relevant parameter determining the range of translational kinetic values for which MBs are trapped, this is the quotient between the dipole–dipole and the stacking coupling constants. The critical kinetic energy increases, or the size of the "trapping window", if this quotient increases.

This paper is organized as follows: In section II, we introduce the interfaced piecewise DNA model and the single inverted dipole DNA model, which includes the long–range interactions and has into account their respective chain conformations. In section III, we investigate the characteristics of the linear modes of the first system, as they are important for determining possible behaviors of MBs when they collide with the interface. It is shown that the linear modes spectrum of this system is similar to the spectrum of a homogeneous DNA molecule with a single inverted dipole. In section IV, we generate numerically MBs which are launched towards the interface and we study the collision phenomena, exploring all the possible scenarios that appear when the translational kinetic energies of the MBs and the coupling parameters are varied. Thereafter, we show that the collisions of MBs in the case of a single inverted dipole DNA molecule, bring about similar effects to the interfaced case. Section V presents some interesting phenomena that can appear when moving breathers collide with a previous trapped breather. Finally, section VI summarizes our results and contains some conclusions.

II. INTERFACED PIECEWISE DNA MODEL

We consider a modification of the Peyrard-Bishop DNA model [2], with the addition of a dipole-dipole energy term. Thus, the Hamiltonian of the system can be written as [24]

$$H = \sum_{n=1}^{N} \left(\frac{1}{2} m \dot{u}_n^2 + D(e^{-bu_n} - 1)^2 + \frac{1}{2} \varepsilon (u_{n+1} - u_n)^2 + \frac{1}{2} \mu \sum_{m \neq n} J_{n,m} u_m u_n \right) \tag{1}$$

The term $\frac{1}{2} m \dot{u}_n^2$ represents the kinetic energy of the nucleotide of mass m at the nth site of the chain, and u_n is

the variable representing the transverse stretching of the hydrogen bond connecting the base at the nth site. The Morse potential, i.e., $D(e^{-bu_n} - 1)^2$, represents the interaction energy due to the hydrogen bonds within the base pairs, being D the well depth, which corresponds to the dissociation energy of a base pair, and b^{-1} is related to the width of the well. The stacking energy is $\frac{1}{2}\varepsilon(u_{n+1} - u_n)^2$, where ε is the stacking coupling constant. The last term of the Hamiltonian, i.e., $\frac{1}{2}\mu \sum_n \sum_{m \neq n} J_{n,m} u_m u_n$, is the long-range dipole–dipole interaction term, where μ is the dipole–dipole coupling constant. The expression for this constant is $\mu = q^2/4\pi\varepsilon_0 d^3$ [24], q being the charge transfer within the dipole and d the distance between neighbouring base pairs, which is supposed to be constant. Finally, $J_{n,m}$ is the dipole-dipole coupling factor given by

$$J_{n,m} = \frac{\alpha_{n,m}}{|m - n|^3},\tag{2}$$

where $|m - n|$ is the normalized distance between base pairs, and $\alpha_{n,m}$ takes the value 1 if the dipoles at n and m are parallel, and -1 if they are antiparallel.

In order to keep the spatial homogeneity in a finite system with periodic boundary conditions [31], the number of particles affected by the long–range interaction must be limited. In consequence, if N is the number of base pairs, we suppose that the long–range interaction affects to $(N - 1)/2$ neighboring base pairs, if N is odd, or $(N - 2)/2$, if N is even, to each direction of a given site of the chain. In fact, we use periodic boundary conditions in a way that both the last dipole and the first one are pointing along the same direction, this implies that the interfaced piecewise chain must has the geometry of a Möbius band, and in this way there exists only one interface in the chain. As an example, we can consider a small system with $N = 8$, with the dipoles located at $n = +1, +2, +3, +4$ pointing in one direction and the other ones located at $n = -1, -2, -3, 0$ pointing in opposite direction. Then, the dipole–dipole coupling factors $J_{n,n+p}$ can be written in a matrix form as follows:

$$\begin{pmatrix}
0 & 1 & 0.1250 & 0.0370 & 0 & 0.0370 & 0.1250 & 1 \\
1 & 0 & 1 & 0.1250 & -0.0370 & 0 & 0.0370 & 0.1250 \\
0.1250 & 1 & 0 & 1 & -0.1250 & -0.0370 & 0 & 0.0370 \\
0.0370 & 0.1250 & 1 & 0 & -1 & -0.1250 & -0.0370 & 0 \\
0 & -0.0370 & -0.1250 & -1 & 0 & 1 & 0.1250 & 0.0370 \\
0.0370 & 0 & -0.0370 & -0.1250 & 1 & 0 & 1 & 0.1250 \\
0.1250 & 0.0370 & 0 & -0.0370 & 0.1250 & 1 & 0 & 1 \\
1 & 0.1250 & 0.0370 & 0 & 0.0370 & 0.1250 & 1 & 0
\end{pmatrix}$$

We perform the following changes of variables:

$$t \rightarrow \omega_0 t, \ u_n \rightarrow bu_n, \ \varepsilon \rightarrow \frac{\varepsilon}{m\omega_0^2}, \ \mu \rightarrow \frac{\mu}{m\omega_0^2}, \ H \rightarrow \frac{H}{2D}, \ D \rightarrow \frac{1}{2},\tag{3}$$

where $\omega_0 = \sqrt{2b^2 D/m}$ is the frequency of an isolated oscillator in the harmonic limit. It becomes unity in the scaled system.

With these changes, the dynamical equations become:

$$\ddot{u}_n + (e^{-u_n} - e^{-2u_n}) + \varepsilon(2u_n - u_{n+1} - u_{n-1}) + \mu \sum_{m \neq n} \frac{\alpha_{n,m}}{|m - n|^3} u_m = 0.\tag{4}$$

III. ANALYSIS OF THE LINEAR MODES

The study of the linear modes (phonons) of a nonlinear discrete system gives a necessary information for predicting some properties of the MBs with a given frequency. For example, the frequencies of MBs must be not too close to the phonon band. Otherwise, they emit a large amount of phonon radiation simultaneously to their movement. Furthermore, as it was shown in [32], the analysis of linear modes allows to predict the scenario of the collisions of MBs with inhomogeneities without the necessity of performing numerical simulations.

The dynamical equations of the interfaced piecewise system can be linearized if we assume that the amplitudes of the oscillations are small enough. Then, the linearized dynamical equations are:
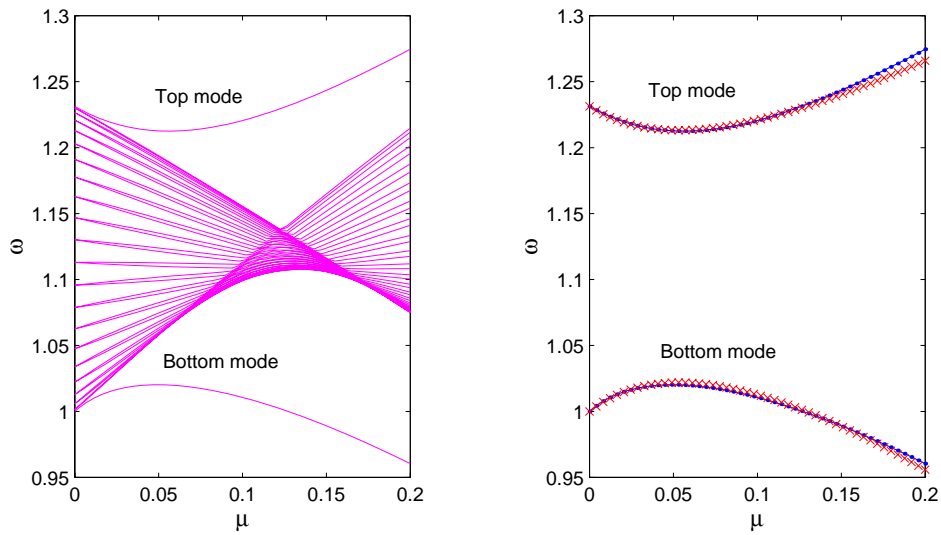
FIG. 2: Left: Frequencies of the linear modes varying the coupling parameter μ for $\varepsilon = 0.129$. The upper line represents the top mode and the lower line represents the bottom mode. Right: Top and bottom mode frequencies with respect to μ. Crosses and dots represent, respectively, analytical and numerical values.

$$\ddot{u}_n + u_n + \varepsilon(2u_n - u_{n+1} - u_{n-1}) + \mu \sum_{p \neq 0} J_{n,n+p} u_{n+p} = 0. \tag{5}$$

The inhomogeneity of these equations determines the existence of two localized modes, one of them is above (top mode) and the other one is below (bottom mode) the extended modes (phonon band).

We have calculated numerically the frequencies of the linear modes for different values of the parameters ε and μ. Fig. 2(left) shows the dependence of the frequency spectrum with respect to the parameter μ for the fixed value of $\varepsilon = 0.129$, which is an appropriate value to obtain MBs with low dispersion [9]. In this figure, it can be observed the existence of localized modes whose origin relies in the fact that the interface acts as an inhomogeneity in the lattice. The localized modes are two, one of them is above (top mode) and the other one is below (bottom mode) the extended modes (phonon band).

The generic profiles of the localized modes are shown in Fig. 3. Their vibration patterns depend on the parameter μ. In particular, we have observed that there exists a critical value μ_c such that for $\mu < \mu_c$, the top mode has a zig-zag vibration pattern, while the bottom mode vibrates in phase. For $\mu > \mu_c$, the vibration patterns are interchanged. As it is shown below, $\mu_c \approx \varepsilon$ (e.g. for $\varepsilon = 0.129$, $\mu_c = 0.123$). This fact is related to the existence of a competition between the attractive (stacking) and the repulsive (dipole–dipole) interaction. The first one is dominant for $\varepsilon \gtrsim \mu_c$ and vice versa.

An approximate explicit expression that gives the dependence of the localized modes frequencies with respect to the coupling constant μ can be obtained considering that the long-range interaction is limited to nearest neighbour base pairs. A study of infinity-range interaction could be performed, but it would be limited to frequencies close to the phonon band [5, 31]. This approximation is justified as the interaction decays rapidly. We have checked that the results are practically coincident except for values of μ far from the ones considered in our study.

The localized modes can be found using Green's lattice function methods [21, 33, 34]. However, the same results can be obtained in a more straightforward way using the following ansatz:

$$\begin{cases} u_n = a_0 r^{|n|} \exp(\mathrm{i}\,\omega\,t) & \text{for } n > 0 \\ u_n = a_1 r^{|n-1|} \exp(\mathrm{i}\,\omega\,t) & \text{for } n < 1 \end{cases}, \tag{6}$$

where r is a spatial decay factor. The sign of r indicates the vibration pattern of the localized mode. If $r > 0$, the particles vibrate in phase, and if $r < 0$, the mode has a zig-zag vibration pattern.

We have supposed that the dipoles at $n \geq 1$ are all antiparallel to the dipoles at $n \leq 0$, then, there exists only two neighboring dipoles which have a different orientation, and the interface is located between $n = 0$ and $n = 1$. As the localized modes are centered between both (see Fig. 3), we assume that:
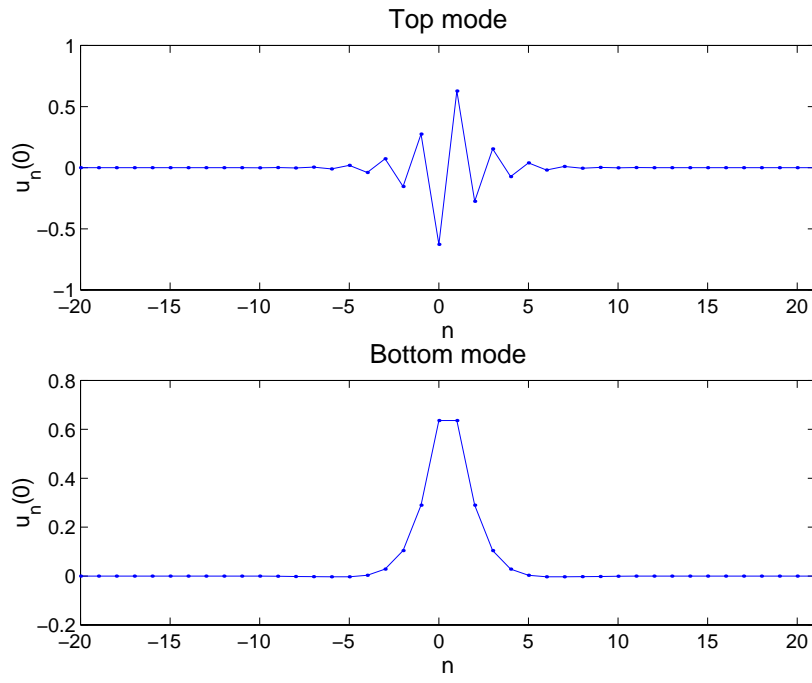
FIG. 3: Generic profiles of the top and bottom localized modes for the coupling values $\mu = 0.05$ and $\varepsilon = 0.129$.

$$\begin{cases} a_0 = -a_1 & \text{(corresponds to the top mode)} \\ a_0 = a_1 & \text{(corresponds to the bottom mode)} \end{cases}. \tag{7}$$

With the application of these ansätze we obtain that the frequencies of the top and bottom modes are, respectively:

$$\omega_{\text{top}}^2 = \omega_0^2 + 2\frac{\mu^2 + 2\varepsilon^2 + \varepsilon\mu}{\varepsilon + \mu} \quad ; \quad \omega_{\text{bottom}}^2 = \omega_0^2 + 2\mu\frac{\varepsilon - \mu}{\varepsilon + \mu}. \tag{8}$$

The decay factors for the top and bottom modes are, respectively:

$$r_{\text{top}} = \frac{\mu - \varepsilon}{\mu + \varepsilon} \quad ; \quad r_{\text{bottom}} = -r_{\text{top}}. \tag{9}$$

¿From these expressions, it is easy to obtain that $\mu_c = \varepsilon$. The discrepancies from this value and the numerical one rely on our assumption that long-range interactions are limited to nearest neighbours. The values of the parameters for which the breather frequency $\omega_{\text{b}} = \omega_{\text{bottom}}$ are related to the scattering properties, see Ref. [32]. However, these values are excluded in our study, because as we require the existence of moving breathers, we need that $\mu < M$ and $\varepsilon > M$, with $M \approx 0.2\omega_{\text{b}}^{2.4}$ [24]. In other words, $\varepsilon > \mu$ is a necessary condition for the existence of moving breathers. The equality $\omega_{\text{b}} = \omega_{\text{bottom}}$ implies that $\mu = [(2\varepsilon - \delta) + \sqrt{4\epsilon^2 + \delta^2 - 8\varepsilon\delta}]/2$, with $\delta \equiv \omega_{\text{b}}^2 - \omega_0^2 < 0$. Thus, it is straightforward to demonstrate that μ must be greater than ϵ in order to get breather resonance with the bottom mode frequency. This region is inaccessible for the moving breathers, as it is shown above.

The analytical and numerical results that give the dependence of the frequencies of the localized modes with respect to μ are represented in Fig. 2(right). As can be appreciated, there is an excellent agreement between the two approaches.

The single inverted dipole system also has two linear localized modes, but now they are localized at the inverted dipole site. The frequencies of these modes are:

$$\omega_{\text{inv}}^2 = \omega_0^2 + 2\varepsilon \pm \frac{2\varepsilon^2 - 4\varepsilon\mu - 14\mu^2}{\sqrt{\varepsilon^2 + 6\varepsilon\mu - 15\mu^2}}. \tag{10}$$

IV. EVOLUTION OF MOVING DISCRETE BREATHERS IN THE INTERFACED PIECEWISE DNA CHAIN.

The dynamics of MBs can be strongly affected by the existence of the interface. It is expected that MBs differing only in their translational kinetic energies can produce different effects when they interact with the interface. In order to study these effects, we have simulated many collisions processes launching MBs towards the interface with different translational kinetic energies.

MBs can be generated numerically by adding to the velocities of a static breather a perturbation of magnitude λ collinear to the pinning mode [15, 16]. The pinning mode is an anti–symmetric linear localized mode, which may appear in the set of linear perturbations of the system when the coupling is strong enough. This perturbation breaks down the translational symmetry of the system and the breather moves with a translational kinetic energy given by $K = \lambda^2/2$. The time evolution of the breathers have been studied using a Calvo's 5th order symplectic algorithm [35].

Recent quantum–mechanical calculations Ref. [36] establishes that in DNA the order of magnitude of the parameter μ is 0.002, therefore, as we are interested in applications to DNA, we have limited our study to this order.

MBs are not exact solutions of the dynamical equations and some phonon radiation is emitted simultaneously to the movement of breathers. This radiation is minimized if the breather frequency is not close to the phonon band. In all the simulations, the breather frequency has been fixed to the value of $\omega_{\rm b} = 0.8$, which is an appropriate value. For smaller values of $\omega_{\rm b}$, the breather gets more and more sharply localized and highly pinned to the lattice, and for $\omega_{\rm b} \lesssim 0.67$ its movement is not possible. Also, phonon radiation increases when the value of the translational kinetic energy increases and some effects due to the size of the system can appear. For that reason the calculations have been tested using different systems sizes, to make sure that the results are not modified by boundary effects (most of the simulations have been done with $N > 200$). The values of the parameter λ have been limited to the interval $(0.01, 0.3)$, as for this interval the phonon radiation is small enough. Finally, the first group of simulations have been done with the value of the stacking coupling constant $\varepsilon = 0.129$.

We have performed a large number of simulations and, essentially, we have found that there exist only two different dynamical regimes, which can be characterized as follows:

Trapping regime :

If the translational kinetic energy of a MB is smaller than a critical value, i.e. $\lambda < \lambda_c$, the breather is trapped at the discontinuity region, that is, only some particles around the interface remain oscillating. The critical translational kinetic energy depends on the values of the parameters μ, ϵ and ω_b. An example of the time evolution of a MB with λ smaller than the critical value, is observed in Fig. 4(a). However, not all the moving breather energy is trapped after the collision because some energy is transferred to the chain as phonon radiation. To see this, we have studied the evolution of the "central energy", i.e. the energy of some few particles around the interface, which is represented in Fig. 5(a). Before the collision the central energy is zero, then it increases quickly taking the value of the incident breather energy, and a small decay of this energy occurs which is due to phonon radiation. This can be appreciated in the central zoom figure of Fig. 5(a).

The analysis of the Fourier spectrum of this trapped breather, carried out after the initial decay of the central energy and at an early stage of the evolution, shows a frequency of value 0.8, which is the internal frequency ω_b of the launched breather, and a frequency of value 0.02, which corresponds to an oscillating movement of the breather around the interface. This type of movement can be appreciated in Fig. 4(a). The absolute values of the Fourier components calculated soon after the collision of the breather with the interface are represented in Fig. 6, and the central energy of this breather has the value 0.7975. The same calculations carried out after a time of 200 breather periods, shows a decrease of the Fourier component corresponding to $\omega = 0.02$, and a central energy of value 0.7943. A very slow–decaying process occurs and the oscillating trapped breather approaches to a static breather centered at the interface with frequency $\omega_b = 0.8$. The energy of this existing static breather is 0.7646. Then, a necessary condition for the trapping effect is the existence of an *inhomogeneity breather solution* (IB) with the frequency of the MB and with a smaller energy. It consists of a static breather solution centered at the inhomogeneity to which the trapped breather decays.

The trapping phenomena for small enough translational kinetic energies, and the oscillatory behavior as a whole of the trapped breather can be partially explained with the help of the collective coordinate method.

In fact, the long–range interaction term of the Hamiltonian may be represented as follows:

$$\frac{1}{2}\mu \sum_n \sum_{m \neq n} J_{n,m} u_n u_m = \sum_n V_n^{Eff} u_n^2 - \frac{1}{4}\mu \sum_n \sum_{m \neq n} J_{n,m}(u_n - u_m)^2, \tag{11}$$

where the first summation term in the rhs represents an effective on-site energy [37], with the on-site potential

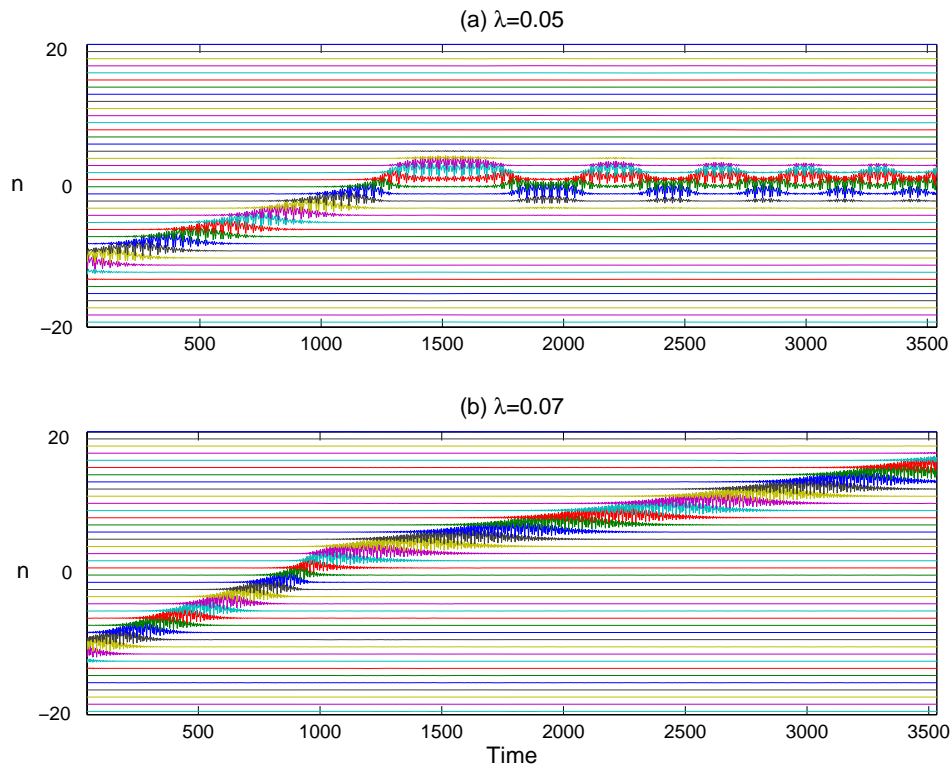FIG. 4: Two different regimes for the interaction of MBs with the interface. Displacement from the n-th equilibrium position versus time, for two different values of the translational kinetic energy: (a) $\lambda < \lambda_c$ and (b) $\lambda > \lambda_c$, with $\mu = 0.002$, $\varepsilon = 0.129$ and $\omega_b = 0.8$. For these parameters values, $\lambda_c = 0.056$. The interface is located between $n = 0$ and $n = 1$.

$$V_n^{Eff} = \frac{1}{2}\mu \sum_{m \neq n} J_{n,m} \tag{12}$$

and the second summation term represents an effective dispersion energy. In the case of a spatially homogeneous system the on-site potential does not depend on the index n, but for the interfaced piecewise system the potential V_n^{Eff}, with $\mu = 0.002$, has the well profile shown in Fig. 7 (dots). It has a symmetric profile, and the depth is close to μ. The DNA chain with a point inhomogeneity given by a single inverted–dipole has an effective potential with the well profile shown in Fig. 7 (open circles). It is also a symmetric profile, and the depth is close to 2μ.

The set of dynamical equations derived from the Hamiltonian (1) can be transformed, in the continuum limit, into the corresponding continuous partial differential equation. Within this context the collective coordinate method provides a good way to analyze the influence of a perturbation on a soliton (in our case we can consider the long range interaction term as a perturbation). The idea is the same as using the center of mass to analyze the behavior of a system of particles. The method introduces the center of the breather "x" as a description variable, and the on-site potential affects as a potential energy of the form

$$V(x) = \frac{1}{2}\mu \sum_n V_n^{Eff} u_{n-x}^2. \tag{13}$$

If the breather is well localized, as occurs in our cases, $V(x) \approx V_x^{Eff}$. In other words, the translational movement of the breather center "x" is affected by a symmetric potential well with the same form as the shown, for each case, in Fig. 7. If the translational kinetic energy of the breather is small enough, the phonon radiation emitted as it passes through the potential well prevents the transmission of the breather and it is trapped with an oscillating movement like a particle in a potential well. The remaining terms in Eq. (11) also contribute to the center of breather motion but they are not so significant. In fact, in the continuum approximation they lead to a space-dependent effective mass of excitation.
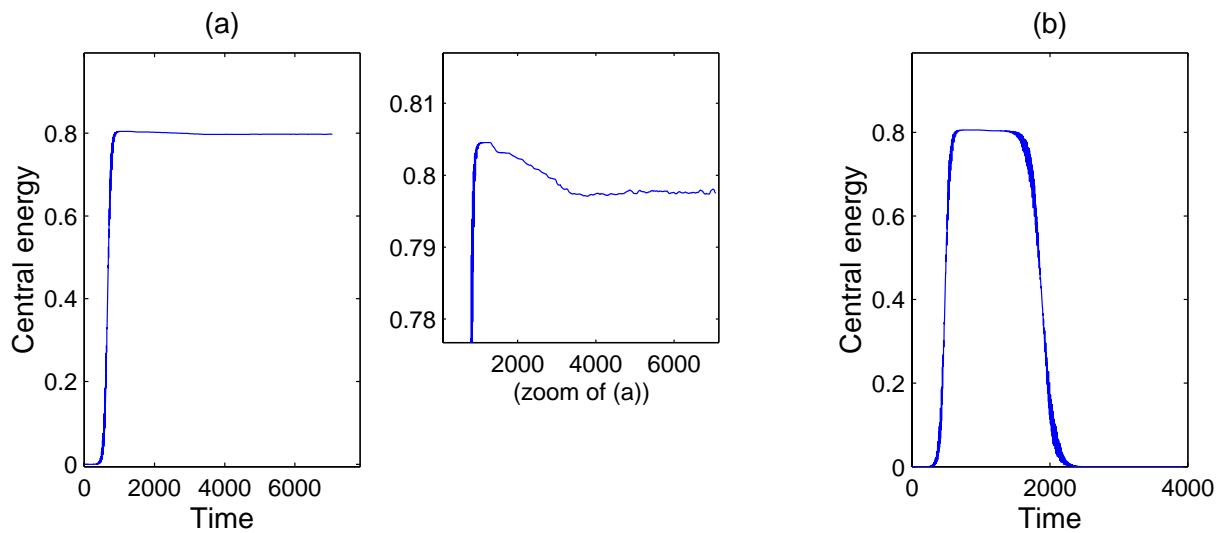
FIG. 5: Time evolution of the central energy corresponding to the collision processes: (a) in Fig. 4(a); (b) in Fig. 4(b). The central figure is a zoom of the left one
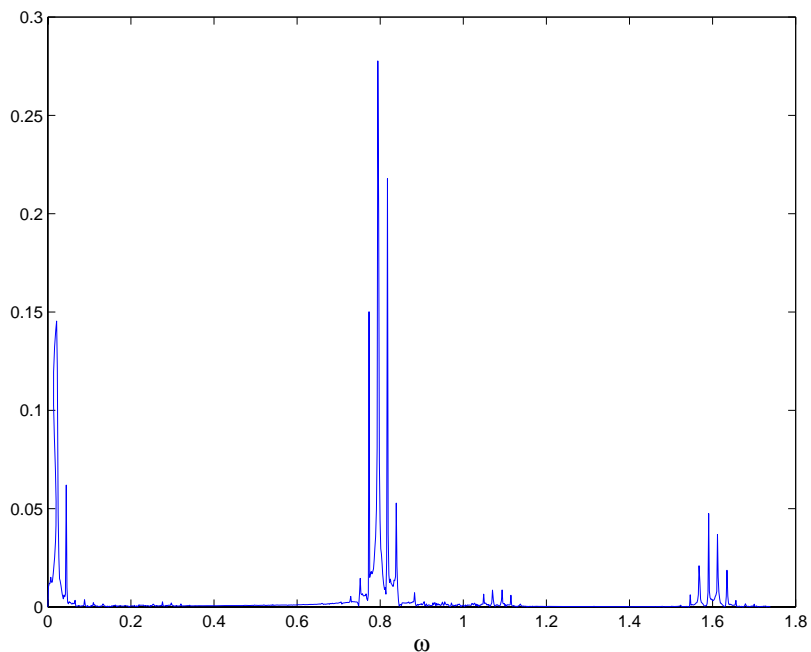

FIG. 6: Absolute values of the Fourier components of the trapped breather shown in Fig. 4(a) calculated soon after the collision

Transmission regime :

If the translational kinetic energy of a MB is bigger than the critical value, i.e. $\lambda > \lambda_c$, the breather crosses the interface and continues its movement along the chain with smaller translational kinetic energy. In other words, the breather is transmitted as a consequence of the interaction with the interface, and a small part of its energy is transferred to the chain as phonon radiation. An example of a transmitted MB can be seen in Fig. 4(b), and the evolution of the corresponding central energy is shown in Fig. 5(b).

The same qualitative results have been found in the case of the parallel-oriented dipole chain with a single inverted–dipole. In this case, the trapping site is centered at the inverted dipole.

Both this system and the interfaced piecewise system have a symmetric effective on–site potential well due to the dipole coupling. Also, both of them have two linear localized modes. The nonexistence of an effective on–site potential
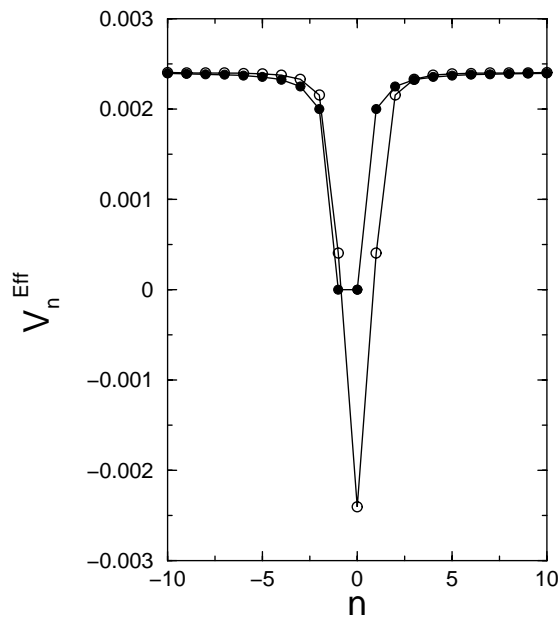
FIG. 7: Effective potential V_n^{Eff}, versus site number, n, for the interfaced piecewise system (dots) and for the single inverted dipole system (open circles).

barrier makes impossible the appearance of a reflection regime.

As mentioned before, the critical value λ_c depends on the values of the parameters μ, ε and the breather frequency ω_b. We have numerically determined the dependence of λ_c with respect to μ for some different values of ε and the fixed value $\omega_b = 0.8$. The results are shown in Fig. 8, where it can be observed that, for a fixed value of ε, λ_c increases monotonously with μ, and, for a fixed value of μ, λ_c decreases monotonously with ε.

Equation (9) shows that the extent of localization of the linear localized modes depends on the values of the parameters μ and ε. In fact, for the interfaced system the decay factor for the bottom mode is given approximately by

$$r_{\text{bottom}} = (1 - \frac{\mu}{\varepsilon})^2. \tag{14}$$

Then, the extent of localization depends basically on the quotient $\kappa = \mu/\varepsilon$. We have observed that varying μ and ε with constant κ, the values of λ_c are practically coincident. Also, when κ increases, or r_{bottom} decreases, λ_c increases. The IB solution is even more localized than the bottom mode because $\omega_b < \omega_{\text{bottom}}$. The values of the critical translational kinetic energies that determine the transitions from the trapping to the transmission regimes are related to the extent of localization of the IB solution. An important result is that for a given system the "trapping window", defined as the range of translational kinetic energy for which trapping occurs, is related to the quotient κ. Higher localization hinders the capability of breathers for being transmitted to the chain.

A similar conclusion can be obtained for the single inverted dipole chain. In this case the values of λ_c are higher than the corresponding to the interfaced chain. For example, with $\mu = 0.002$ and $\epsilon = 0.129$ we obtain $\lambda_c = 0.195$. With the same value of ϵ and with $\mu = 0.0025$, $\lambda_c > 0.3$, although this value is out of the interval of λ values that we have considered in this paper.

The problem of the interaction of MBs with an impurity in a homogeneous Klein-Gordon chain was considered in [32]. In that case MBs can be reflected, trapped or transmitted by the impurity, and a necessary condition for the appearance of trapping is the existence of an impurity breather solution, that is, a static breather solution centered at the impurity. Similarly, we have seen that for our systems a necessary condition for trapping is the existence of an *inhomogeneity breather solution* (IB) with the frequency of the MB and an internal energy smaller than the internal energy of the MB.

Fig. 9 shows that, for $\epsilon = 0.129$ and $\omega_b = 0.8$, the difference between the inhomogeneity breather energy (E_{IB}) and the internal energy of the moving breather (E_{MB}) is negative. This confirms the existence of inhomogeneity breathers and that its energy is smaller than the moving breather energy, which is the necessary condition for trapping.
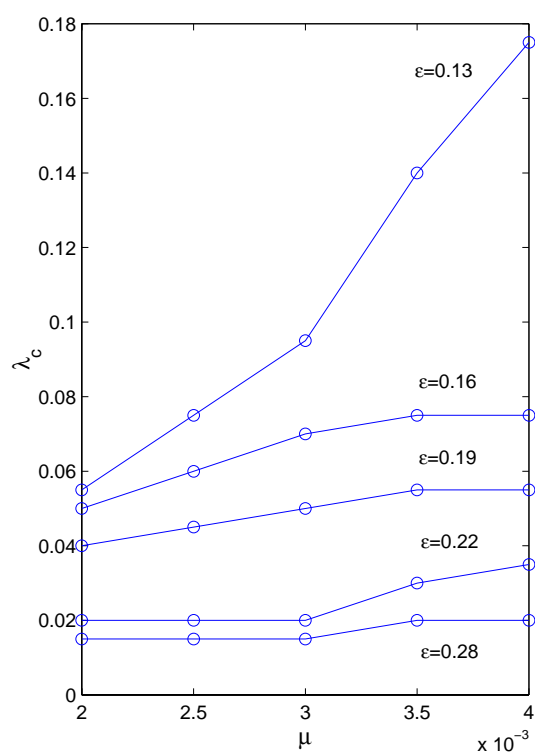
FIG. 8: Dependence of λ_c with respect to μ for some different values of ε.

It can also be observed in this figure that the magnitude the difference between the inhomogeneity breather energy (E_{IB}) and the internal energy of the moving breather (E_{MB}) increases monotonously with μ. Thus, the phonon radiation emitted by a trapped breather increases with μ.

V. ENERGY ACCUMULATION AT THE INTERFACE REGION: BREATHER COLLISIONS.

The study of the trapping of several breathers at the interface region is of great interest. When a MB is trapped, other incoming breathers can also be trapped after colliding with the interface. This process could increase the energy density locally, thus collecting or accumulating energy in the interface region. Another point of interest is whether there is a saturation threshold for this accumulated energy .

In general, the study of energy exchange in collisions of MBs is a difficult problem. Some results are known for a special type of FPU lattice [38], and in a one–dimensional DNA model [39], but at present no general results are known concerning to collisions of MBs in Klein–Gordon lattices.

The simulations show that when a MB collides with a trapped breather, the effects of the collision are strongly dependent on their exact dynamical details when the effective collision processes begin. We have performed a large number of simulations in a chain of N=200 base pairs, with the coupling parameters $\mu = 0.002$ and $\epsilon = 0.129$. All the breathers have the frequency $\omega_b = 0.8$. We have found that under favorable conditions the accumulation of energy is possible as a consequence of the trapping of successive breathers.

We show in Fig. 10(a) contour plots for the evolution of the energy density of five breathers launched towards the interface at different instant of time. All the translational kinetic energies are different.

The first breather is launched towards the interface at $t = 0$ with a translational kinetic energy smaller than the critical value, $(\lambda_c = 0.056)$, so that the breather is trapped at the discontinuity region.

The phonon radiation must be removed because it distorts the numerical simulations when it is reflected at the boundaries. For that purpose, just before each breather is launched, we set to zero the displacements and velocities outside the interface region, $(|n| > 5)$.

The second breather is launched with $\lambda = 0.07$, which is greater than λ_c, but it is also trapped at the interface. We have observed that the results of the collision between these two breathers depends strongly on their relative phase when the collision processes begin. We have chosen the translational kinetic energy of this second breather in order to obtain an efficient trapping.
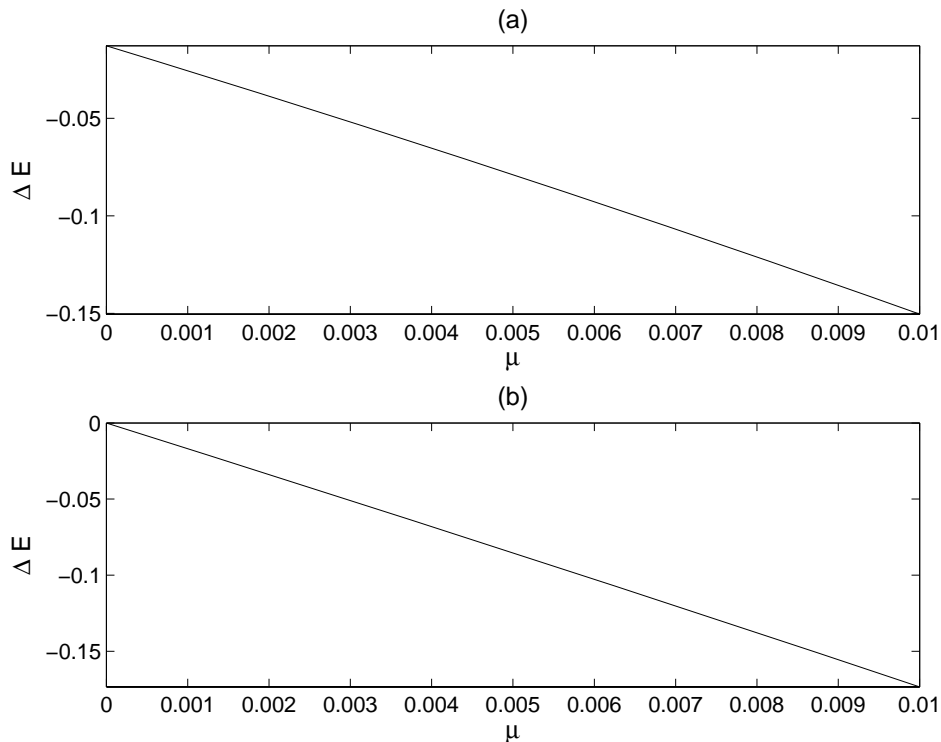
FIG. 9: Dependence of the difference between the inhomogeneity breather energy (E_{IB}) and the internal energy of the moving breather (E_{MB}) with respect to μ, for $\epsilon = 0.129$ and $\omega_b = 0.8$. (a) the interface case, (b) the single inverted–dipole case

Using the same procedure as before, three consecutive breathers are launched with $\lambda = 0.15; 0.19; 0.2$, respectively. All of them are trapped, and to illustrate the evolution of the total collected energy at the interface, we have represented in Fig. 10(b) the central energy versus time. We observe that after each collision the total trapped energy increases, but only part of the energy of each incident breather is accumulated at the interface region. The numerical simulations show that the breather is partly transmitted and partly reflected, and also some little phonon radiation appears. It is interesting to observe that the phonon radiation increases as the number of trapped breathers or the energy accumulated increases. The possibility for trapping more energy at the inhomogeneity region by additional incoming breathers seems to have a limit due to a saturation effect.

The accumulation of energy at the interface region could start local base pair openings in the DNA molecule. Nevertheless, the simulations show that the accumulation of energy can, occasionally, disappears after an appropriate collision. An example of this is shown in Fig. 11, where the last collision induces the transmission of the accumulated energy to the right side of the chain. In this simulation five breathers are launched successively towards the interface with $\lambda = 0.05$, $\lambda = 0.07$, $\lambda = 0.15$, $\lambda = 0.18$ and $\lambda = 0.14$, respectively.

To gain deeper insight into the possible reasons for these striking features, the authors are currently investigating this issue and will be object of a future work.

VI. CONCLUSIONS

We have studied the evolution, and some collision processes, of MBs in two different DNA molecules. The first DNA chain consists of a sequence of identical base pairs, where there exists an interface such that the dipole moments at each side are oriented in opposite directions. The second chain consists also of a sequence of identical base pairs but there exists a single dipole moment which is oriented in opposite direction to that of the others ones. I both cases there exists a local inhomogeneity defined by the interface or the single inverted dipole, respectively.

The Hamiltonian of the Peyrard–Bishop model is augmented with an energy term that takes into account the long–range forces due to the dipole–dipole coupling between the base pairs. We have generated MBs with different translational kinetic energies and studied the effects of the collisions with the interface or with the single inverted dipole, respectively. In each case, the outcome depends on the values of the stacking coupling constant, the dipole–
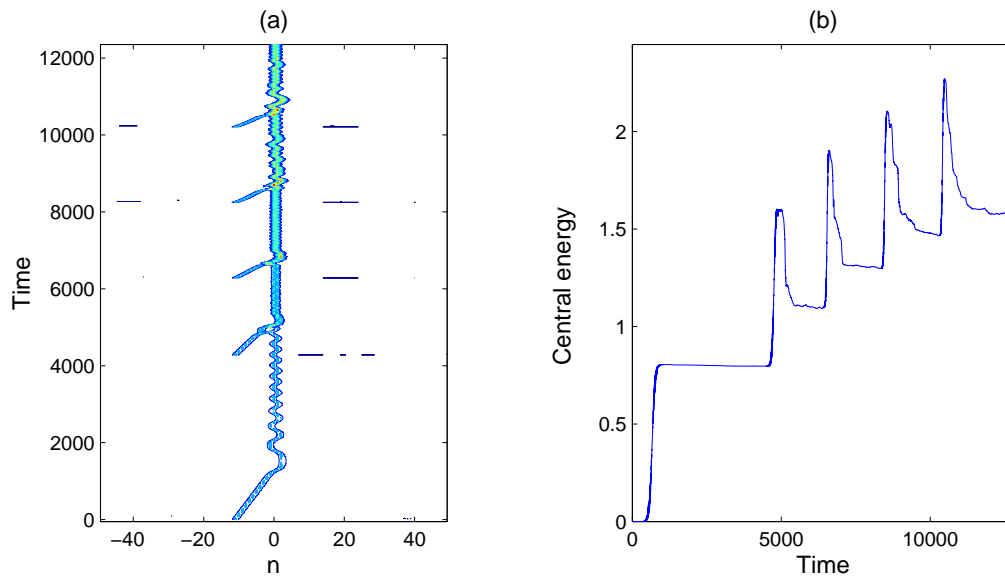
FIG. 10: (a) Contour plots for the evolution of five breathers launched towards the interface with different translational kinetic energies. The breathers are trapped at the interface increasing the accumulated energy density ($\lambda = 0.05; 0.07; 0.15; 0.19; 0.2$). (b) Time evolution of the central energy.
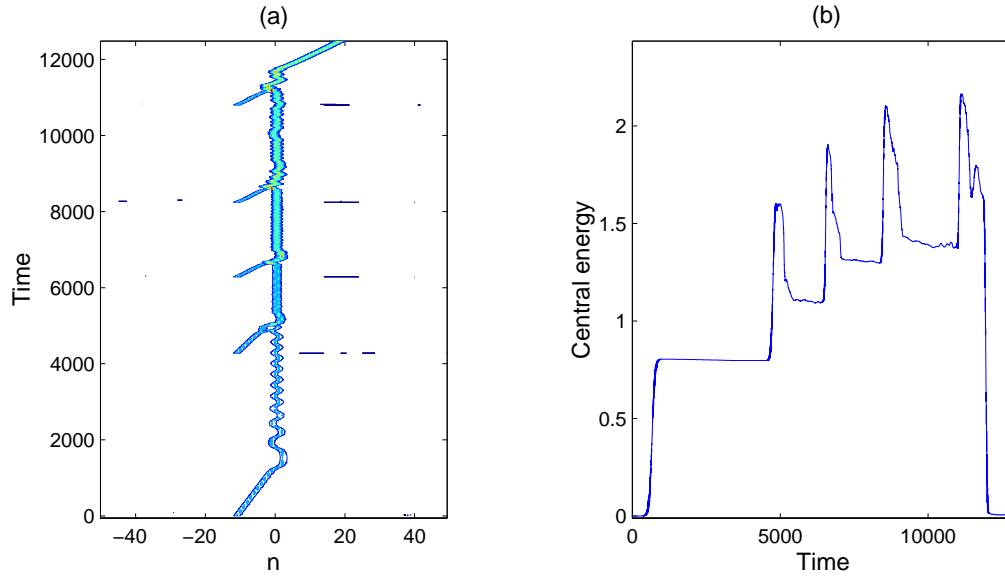

FIG. 11: (a) Contour plots for the evolution of five breathers launched towards the interface, with different translational kinetic energies ($\lambda = 0.05; 0.07; 0.15; 0.18; 0.14$). After the last collision the accumulated energy is transmitted to the right side of the chain. (b) Time evolution of the central energy.

dipole coupling constant, the frequency and the translational kinetic energy of the MBs. Taking fixed values for the first three quantities, we have found that if the kinetic energy of the MB is smaller than a critical value, the breather is trapped after colliding with the interface, whereas if the kinetic energy is larger, the breather is transmitted to the other side of the interface loosing energy. Therefore, there exist two different dynamical regime: a) the trapping regime, when MBs are trapped at the interface; b) the transmission regime, when MBs are transmitted to the other side of the interface. The same effects appear when MBs collide with a single inverted dipole in the chain. In both cases, a necessary condition for the trapping of a MB is the existence of a stationary breather solution with the

same frequency, centered at the inhomogeneity site, which we call inhomogeneity breather (IB), and with a smaller energy than the internal energy of the MB. When collision occurs part of the energy is transferred to the chain as phonon radiation. The existence, for each case, of a symmetric effective on–site potential well due to the dipole-dipole coupling, explains qualitatively the found behavior.

The value of the critical translational kinetic energy that determines the transition from the trapping regime to the transmission regime is directly related to the extent of the localization of the IB. This extent of localization is related to the quotient between the long–range and the short–range coupling parameters. Trapping or accumulation of energy is facilitated when this quotient increases.

It is important to state that the most simple structural modification in a homogeneous DNA molecule, which is to reverse the orientation of a single dipole, provides a mechanism for the trapping of moving breathers. The simulations show that some incoming MBs can also be trapped after colliding with a trapped breather, producing an accumulation of energy at the inhomogeneity region. The interface or the inverted dipole can play the role of chargers of vibrational energy. Occasionally, a successful incoming breather can collide with this excited region and all the accumulated energy can be carried away to the rest of the DNA chain. At this point, if these processes occur really in nature, one is tempted to imagine that succsesive pulses of accumulated energy can arrive to a coding sequences producing the initiation of the transcription processes. The design of experiments in real or synthetic DNA are encouraged in order to verify the results presented in this paper.

[1] L. Yakusevich, *Nonlinear Physics of DNA*, Wiley series in nonlinear sciences (John Wiley & sons, Weinheim, 2004).
[2] M. Peyrard and A. Bishop, Phys. Rev. Lett. **62**, 2755 (1989).
[3] V. Danilov and V. Anisimov, Journal of Biomolecular Structure and Dynamics **22**, 471 (2005).
[4] D. Jose and D. Porschke, Nucleic Acids Res. **32**, 2251 (2004).
[5] Y. Gaididei, S. Mingaleev, P. Christiansen, and K. Rasmussen, Phys. Rev. E **55**, 6141 (1997).
[6] S. Mingaleev, P. Christiansen, Y. Gaididei, M. Johansson, and K. Rasmussen, J. Biol. Phys. **25**, 41 (1999).
[7] J. Archilla, P. Christiansen, S. Mingaleev, and Y. Gaididei, J. Phys. A: Math. and Gen. **34**, 6363 (2001).
[8] J. Archilla, P. Christiansen, and Y. Gaididei, Phys. Rev. E **65**, 016609 (2001).
[9] J. Cuevas, F. Palmero, J. Archilla, and F. Romero, Phys. Lett. A **299**, 221 (2002).
[10] P. Larsen, P. Christiansen, O. Bang, J. Archilla, and Y. Gaididei, Phys. Rev. E **69**, 026603 (2004).
[11] P. Larsen, P. Christiansen, O. Bang, J. Archilla, and Y. Gaididei, Phys. Rev. E **70**, 036609 (2004).
[12] S. Aubry, Physica D **103**, 201 (1997).
[13] S. Flach and C. R. Willis, Phys. Rep. **295**, 181 (1998).
[14] R. MacKay, Physica A **288**, 175 (2000).
[15] D. Chen, S. Aubry, and G. P. Tsironis, Phys. Rev. Lett. **77**, 4776 (1996).
[16] S. Aubry and T. Cretegny, Physica D **119**, 34 (1998).
[17] T. Cretegny, Ph.D. thesis, École Normale Supérieure de Lyon (1998).
[18] J. Marín, J. Eilbeck, and F. Russell, Phys. Lett. A **248**, 225 (1998).
[19] J. Marín, J. Eilbeck, and F. Russell, in *Nonlinear Science at the dawn of the 21st century*, edited by P. Christiansen and M. Soerensen (Springer, 2000), p. 293.
[20] J. Marín, F. Russell, and J. Eilbeck, Phys. Lett. A **281**, 21 (2001).
[21] T. Dauxois, M. Peyrard, and C. Willis, Physica D **57**, 267 (1992).
[22] T. Dauxois, M. Peyrard, and A. Bishop, Phys. Rev. E **47**, 684 (1993).
[23] M. Gueron, M. Kochoyan, and J. Leroy, Nature **328**, 89 (1987).
[24] J. Cuevas, J. Archilla, Y. Gaididei, and F. Romero, Physica D **163**, 106 (2002).
[25] K. Forinash, M. Peyrard, and B. Malomed, Phys. Rev. E **49**, 3400 (1994).
[26] M. Hisakado, Phys. Lett. A **227**, 87 (1997).
[27] K. Baverstock, Int. J. Radiat. Biol. **47**, 369 (1985).
[28] G. S. B Suter and F. Thoma, Nucleic Acids Res. **28**, 4083 (2000).
[29] K. Kleppe, E. Ohtsuka, R. Kleppe, I. Molineux, and H. Khorana, J. Mol. Biol. **56**, 341 (1971).
[30] Y. Z. KA Marx and I. Kishawi, Journal of Biomolecular Structure and Dynamics **23**, 429 (2006).
[31] S. Flach, Phys. Rev. E **58**, R4116 (1998).
[32] J. Cuevas, F. Palmero, J. F. R. Archilla, and F. R. Romero, J. Phys. A: Math. and Gen. **35**, 10519 (2002).

[33] O. Braun and Y. Kivshar, Phys. Rev. A **43**, 1060 (1991).

[34] A. Maradudin, E. Montroll, and G. Weiss, *Theory of lattice dynamics in the harmonic approximation* (Academic Press, Nueva York, 1963).

[35] J. Sanz-Serna and M. Calvo, *Numerical Hamiltonian problems* (Chapman and Hall, 1994).

[36] J. Cuevas, E. Starikov, J. Archilla, and D. Hennig (2004), submitted, `arXiv:nlin.PS/0404029`.

[37] Y. Gaididei, S. Mingaleev, and P. Christiansen, Phys. Rev. E **62**, R53 (2000).

[38] Y. Doi, Phys. Rev. E **68**, 066608 (2003).

[39] J. Ting and M. Peyrard, Phys. Rev. E **53**, 1011 (1996).